Available online at www.sciencedirect.com
ScienceDirect
Journal of Power Sources 177 (2008) 464–469
JOURNAL OF POWER SOURCES
www.elsevier.com/locate/jpowsour

Short communication

Electrical properties of Al-doped oxyapatites at intermediate temperature

Sami Chefi [a,*], Adel Madani [a], Hedi Boussetta [a], Claude Roux [b], Abdelkader Hammou [b]

[a] *Laboratoire de Physique des Matériaux, Faculté des Sciences de Bizerte, Zarzouna 7021, Tunisia*
[b] *Laboratoire d'Electrochimie et de Physico-chimie des Matériaux et des Interfaces (INPG, CNRS et UJF) 1130, rue de la Piscine, B.P75, 38402 Saint Martin d'Hères CEDEX, France*

Received 20 September 2007; received in revised form 16 November 2007; accepted 29 November 2007
Available online 5 December 2007

Abstract

In order to obtain acceptable performances in SOFC, relatively high operating temperatures (∼850–1000 °C) are required. That is mainly due to the low ionic conductivity of YSZ electrolyte. These temperature conditions are at the origin of the cell degradation, which justify the search for alternative electrolytes presenting the same performances but at lower temperature (∼800 °C). It is in this context that the oxyapatites of general formula $La_{10-x}Si_{6-y}Al_yO_{27-3x/2-y/2}$ ($x = 0, 0.67$; $y = 0.25, 0.50, 0.75$) are studied in this work. The solid solutions are prepared by sintering the oxide powders at 1600 °C. All samples have shown a hexagonal structure with an increase in the cell parameters with the aluminium content. Electrical properties are determined by impedance spectroscopy between 169 and 790 °C. The results are treated by separating the bulk and grain boundary conductivities between 169 and 500 °C and in the form of total (bulk + grain boundary) conductivity between 500 and 790 °C. The respective influences of the activation energy and the pre-exponential factor on conductivity are analyzed. Activation energies are about 0.65 eV suggesting an interstitial mechanism. No variation of conductivity is observed with the oxygen partial pressure. Finally, $La_{10}Si_{5.5}Al_{0.5}O_{26.75}$ shows conductivity higher than that of YSZ at intermediate temperature.

Keywords: Oxyapatites; SOFC; Ionic conduction; Impedance spectroscopy

1. Introduction

Taking into account their high efficiency, SOFC (solid oxide fuel cells) are regarded as promising devices for the electrochemical energy conversion. Yttria-stabilized zirconia (YSZ), with general formula $(ZrO_2)_{1-x}(Y_2O_3)_x$, is currently used as electrolyte in these fuel cells. This material has remarkable properties in terms of chemical, structural and thermal stability. However, its low ionic conductivity requires the use of relatively high operating temperatures (850–1000 °C) to obtain acceptable performances. Moreover, the manufacturing processes of the SOFC imply the deposition of the $La_{1-x}Sr_xMnO_3$ cathode at high temperature. A chemical reactivity with the YSZ electrolyte may take place at the interface with the formation of highly resistive phases. In order to solve these problems, research was undertaken to find other electrolytes showing comparable properties as YSZ but at lower temperature (≈800 °C). The ceria-based solid solutions, i.e. $(CeO_2)_{1-x}(Gd_2O_3)_x$ as well as the BIMEVOX (bismuth–vanadium oxides) proved to be unusable because of their gradual electrochemical reduction in the presence of hydrogen or methane [1,2]. La_2O_3-based solid solutions are sensitive to steam and to CO_2 produced at the fuel cell anode when reformed methane is oxidized. Finally, poor stability and conductivity performances were revealed with the electrolytes based on lanthanum gallates [3]. During the last 10 years, a new family of oxide conducting solid electrolytes, the oxyapatites of general formula $A_{10-x}(MO_4)_6O_{2\pm d}$ with M = Si, Ge and A = rare earth, alkaline earth [4] have attracted large attention due to their conductivity comparable to YSZ at moderate temperature [5]. An interesting and concise description of their properties is given in the introductive part of Shaula et al.'s work [6]. Studies of doped oxyapatites have shown that to achieve high conductivitiy in these materials, non-stoichiometry in the form of either cation vacancies or oxygen excess is required [7–9]. So conductivity enhancements were reported for substitution of trivalent cations B^{3+} and Ga^{3+} [10], Al^{3+} [6] for Si^{4+}.

The main objective of the present work is to measure the bulk and grain boundary conductivity in the Al-doped

* Corresponding author. Tel.: +216 72591906; fax: +216 72590566.
E-mail address: chefisami@yahoo.fr (S. Chefi).

0378-7753/$ – see front matter © 2007 Elsevier B.V. All rights reserved.
doi:10.1016/j.jpowsour.2007.11.091

oxyapatites $La_{10-x}Si_{6-y}Al_yO_{27-3x/2-y/2}$. The undoped sample $La_{9.33}Si_6O_{26}$ was studied in the same conditions and considered as a reference for comparison with Al-doped oxyapatites.

2. Experimental procedure

High purity La_2O_3, SiO_2 (Prolabo 99.9%) and Al_2O_3 (Baikalox 99.9%) powders were used to prepare a series of Al-doped samples: $La_{10-x}Si_{6-y}Al_yO_{27-3x/2-y/2}$ ($x = 0$, 0.67; $y = 0.25$, 0.50, 0.75). Before weighting, La_2O_3 and SiO_2 powders were dried at 1000 °C and 1200 °C, respectively for 1 h. The powders with stoichiometric ratios were mixed, grounded with ethanol in equal quantity [11] and calcinated at 1500 °C for 2 h. The calcinated powders were grounded using attrition procedure and uni-axially pressed as pellets. Finally, these pellets were isostatically pressed at 2500 bar and sintered at 1600 °C for 3 h in air. To determine the samples crystallographic structure, X-ray diffraction analysis (XRD) was performed at room temperature with a Pan Analytical diffractometer using Cu Kα_1 radiation.

Experimental densities were determined using a pycnometer with distilled water. Density values were calculated using the following expression:

$$\rho_{exp} = \left[\frac{M_1 - M_0}{(M_3 - M_0) - (M_2 - M_1)}\right](\rho_{dw} - \rho_{air}) + \rho_{air} \quad (1)$$

where M_0 represents the pycnometer weight, M_1 the weight of the sample with the pycnometer, M_2 the weight of pycnometer with distilled water and the sample, and M_3 the weight of the water, ρ_{air} the density of air and ρ_{dw} the density of distilled water.

Microscopic examinations were performed using a Jeol JSM.6400 scanning electron microscope.

Electrical properties were measured between 169 and 790 °C, using Hewlett-Packard HP 4192 analyzer in the frequency range 5 Hz–13 MHz and an Autolab analyzer in the frequency range 10 mHz–1 MHz. A symmetrical cell was used, using Pt paste electrodes painted and fired at 900 °C for 1 h in air on both faces of the pellet. To determine the oxygen partial pressure PO_2 dependence of the conductivity, experiments were carried out with PO_2 varying from air down to about 10^{-21} atm, using O_2–Ar mixtures and H_2–H_2O mixtures. An oxygen electrochemical pump was used to monitor PO_2. An oxygen zirconia sensor, working at 700 °C with air as a reference, was used to measure PO_2 in the gaseous mixtures to be introduced in the experimental chamber.

3. Results and discussion

3.1. Microstructural characterization

Diffraction diagrams in Fig. 1 indicate that no secondary phase was detected and that all samples have an apatite-type hexagonal structure. As seen in Table 1, lattice parameters are influenced similarly by Al and La contents. For the undoped $La_{9.33}Si_6O_{26}$ sample, our XRD results are consistent with those previously published [5]. At fixed La content, the unit cell volume increases with incorporation of Al^{3+} due to its larger radius with respect to Si^{4+} ($r^{3+}_{Al} = 0.53$ Å , $r^{4+}_{Si} = 0.40$ Å). The

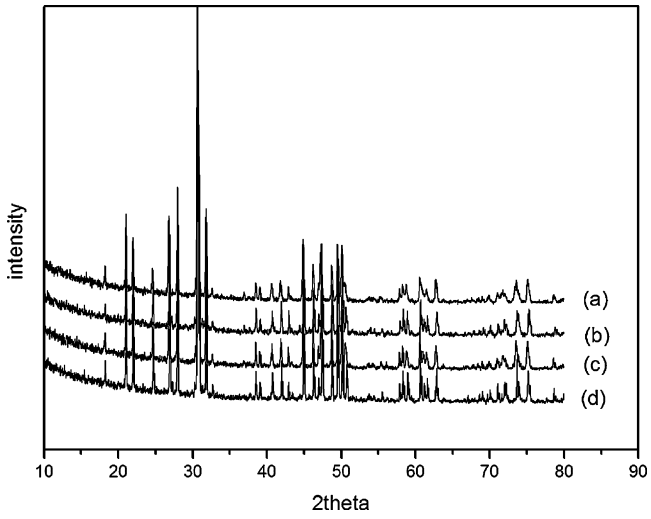

Fig. 1. XRD spectra of oxyapatites: $La_{10}Si_{5.5}Al_{0.5}O_{26.75}$ (a), $La_{10}Si_{5.75}Al_{0.25}O_{26.87}$ (b), $La_{9.33}Si_{5.25}Al_{0.75}O_{25.62}$ (c), $La_{9.33}Si_6O_{26}$ (d).

Table 1
Lattice parameters of oxyapatite samples

Samples	$a = b$ (Å)	c (Å)	V (Å)^3	Reference
$La_{9.33}Si_6O_{26}$	9.72533	7.18952	588.87	This work
$La_{10}Si_{5.75}$ $Al_{0.25}O_{26.87}$	9.70810	7.19401	587.16	–
$La_{10}Si_{5.5}$ $Al_{0.5}O_{26.75}$	9.73242	7.22696	592.80	–
$La_{9.33}Si_{5.25}$ $Al_{0.75}O_{25.62}$	9.73343	7.21682	592.10	–
$La_{9.33}Si_6O_{26}$	9.721	7.187	588.20	[5]

c parameter of the hexagonal structure is more affected than the a and b parameters.

Table 2 summarizes the picnometry results with a measured relative density varying between 91.8% and 94.9%. Despite the high sintering temperature, the synthesized oxyapatites exhibit a relatively low density. Micrographs of the sintered materials are shown in Fig. 2. An average grain size of 2.5 μm can be estimated, and no significant differences in microstructure are observed between the different compositions. These micrographs confirm picnometry results in term of low density mainly due to the existence of closed microporosity.

3.2. Electrical conductivity

According to the impedance response of the cell, the investigated temperature range is divided into the two following domains:

Table 2
Theoretical (XRD) and measured (picnometry) density of the investigated oxyapatites

Sample composition	Theoretical density (g cm^{-3})	Experimental density (g cm^{-3})	Relative density (%)
$La_{10}Si_{5.75}$ $Al_{0.25}O_{26.87}$	5.61	5.24	93.4
$La_{10}Si_{5.5}$ $Al_{0.5}O_{26.75}$	5.55	5.27	94.9
$La_{9.33}Si_{5.25}$ $Al_{0.75}O_{25.62}$	5.29	4.96	93.7
$La_{9.33}Si_6O_{26}$	5.30	4.87	91.8

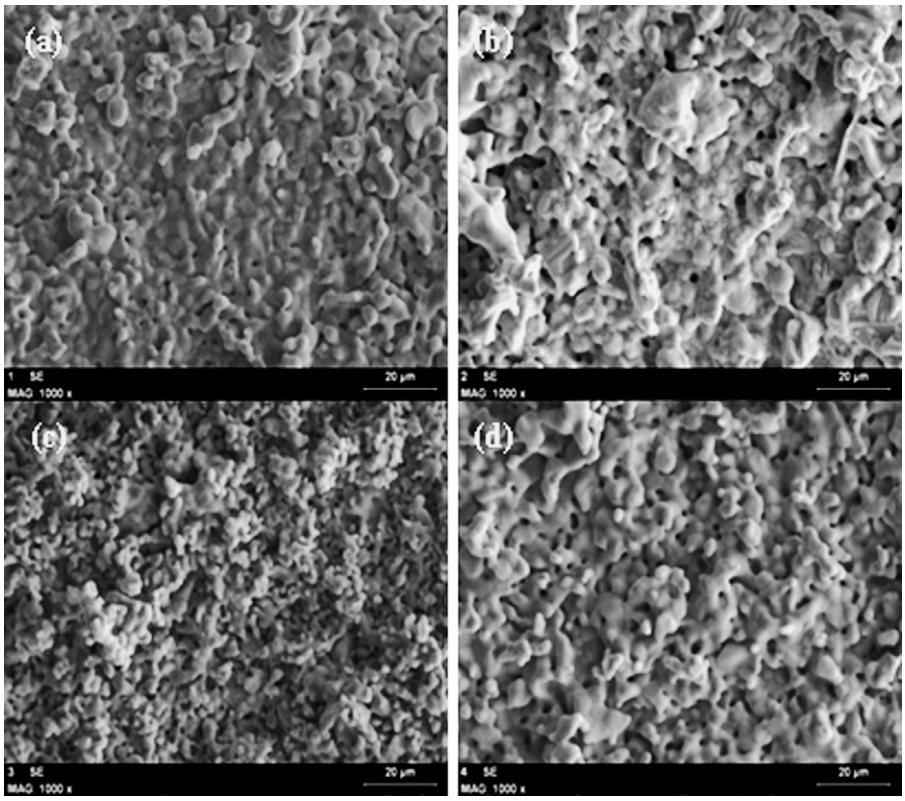

Fig. 2. SEM micrograph of oxyapatite ceramics: $La_{10}Si_{5.75}Al_{0.25}O_{26.87}$ (a), $La_{10}Si_{5.5}Al_{0.5}O_{26.75}$ (b), $La_{9.33}Si_{5.25}Al_{0.75}O_{25.62}$ (c), $La_{9.33}Si_6O_{26}$ (d).

a) $169\,^{\circ}C \leq T \leq 500\,^{\circ}C$
b) $500\,^{\circ}C \leq T \leq 790\,^{\circ}C$

Within the (a) domain, the impedance spectrum is mostly representative of the mass electrical properties of oxyapatites. Bulk and grain boundary contributions are easily separated. Typical impedance diagram of this domain is shown in Fig. 3 at 257 °C. The bulk response is associated with the semicircle at high frequencies and the intermediate frequency range with the grain-boundaries contribution. The impedance response associated with the electrode is recorded at lower frequencies and results are not sufficient for an accurate description of the related electrical phenomena. Using Zview software [12], impedance spectra were fitted satisfactorily with a parallel R-CPE circuit model and R was extracted. The CPE value is approximately 10^{-10} F and 10^{-7} F for the bulk and grain boundary, respectively. Bulk and grain boundary conductivities, σ_b and σ_{gb}, respectively, were calculated using the following relation:

$$\sigma_i = \frac{1}{R_i}\frac{l}{S} \tag{2}$$

R_i (i = b, gb) is the resistance obtained from impedance diagrams and S and l are the area and the thickness of the sample, respectively. The temperature dependence of bulk and grain boundary conductivities is represented in Figs. 4 and 5, respectively. A linear variation is observed in Arrhenuis plots,

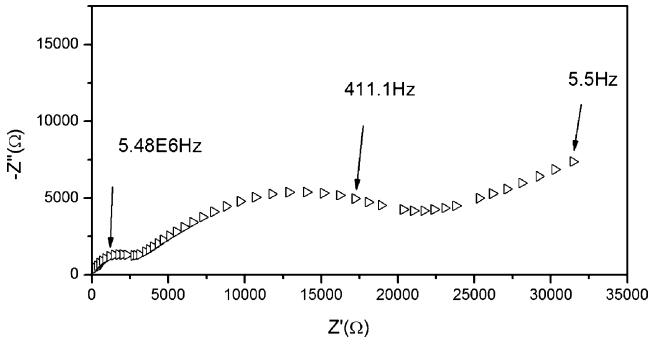

Fig. 3. Typical impedance diagram of $La_{10}Si_{5.5}Al_{0.5}O_{26.75}$ at 257 °C.

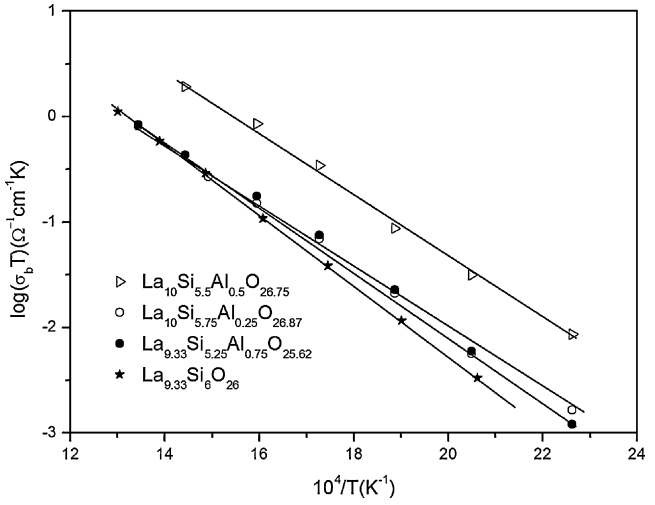

Fig. 4. Temperature dependence of the bulk conductivity of oxyapatite in air.

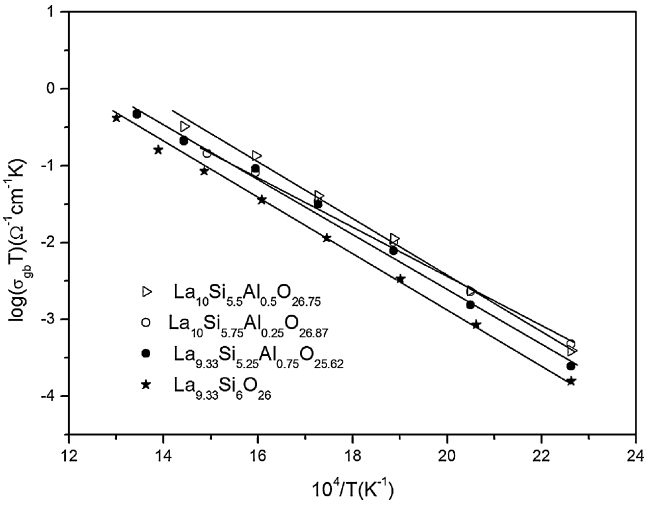

Fig. 5. Temperature dependence of the grain boundary conductivity of oxyapatite in air.

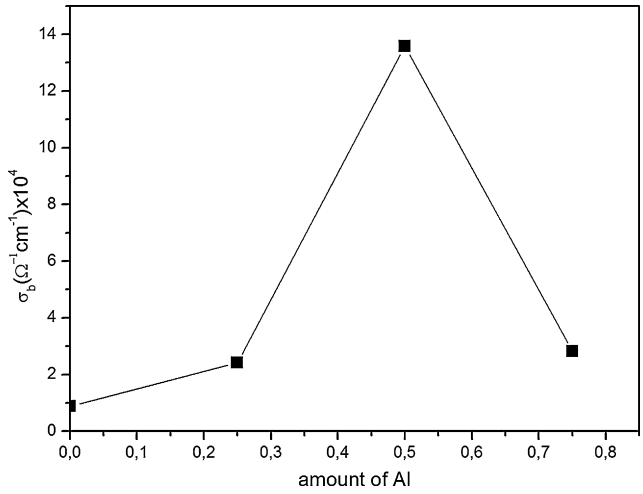

Fig. 6. The variation of the bulk conductivity as a function of Al-content at 350 °C.

following the relation:

$$\sigma = \sigma_0 \exp\left(\frac{-E_a}{kT}\right) \quad (3)$$

where E_a is the activation energy and k the Boltzmann constant. The usual treatment [13–15] of ionic conductivity describes the motion of charge carrier through the lattice with an equation of the form:

$$\sigma = \frac{\upsilon l^2 e^2 C}{kT} \exp\left(-\frac{E_a}{kT}\right) \quad (4)$$

with $A = Ce^2\upsilon l^2/k$and where υ the jump frequency, l is the interatomic jump distance, e the charge number of the mobile ion and C is a constant related to concentration, geometric and entropy effects associated to charge carriers.

Table 3 shows bulk and grain boundary activation energy of electrical conductivity for different compositions. A slight decrease of the activation energy value is observed with Al-doping. This value is significantly lower than that associated with YSZ [16] and close to that observed with ceria-based solid solutions [17]. For a given composition, this parameter is systematically higher for the grain boundary conductivity. Such a behaviour has already been observed in the case of oxide conducting electrolytes [18–20]. According to literature, the high resistance of the boundaries may be due to various reasons, including impurity segregation, secondary phases, pore trapping and local ordering.

Table 3
Activation energy of the bulk and grain boundary conduction for the investigated oxyapatites

Sample composition	Temperature range (°C)	E_a(eV)	
		Bulk	Grain boundary
$La_{9.33}Si_6O_{26}$	$169 < T < 496$	0.64	0.68
$La_{10}Si_{5.75}Al_{0.25}O_{26.87}$	$169 < T < 471$	0.58	0.63
$La_{10}Si_{5.5}Al_{0.5}O_{26.75}$	$169 < T < 420$	0.60	0.71
$La_{9.33}Si_{5.25}Al_{0.75}O_{25.62}$	$169 < T < 471$	0.61	0.70
9.5%YSZ [16]	$350 < T < 540$	1.15	1.18
$La_{9.33}Si_6O_{26}$ [8]	$84 < T < 441$	0.8	–

In the following, conductivity results are analysed through activation energy and pre-exponential factor A variation versus composition. Figs. 6–8 show the variation of the bulk conductivity, the activation energy and the pre-exponential factor as a function of Al-content. A maximum of conductivity appears for the composition corresponding to 0.5 aluminium atom per formula unit. This maximum does not correspond to the lowest activation energy but to the highest pre-exponential factor. These two factors do not act in the same way to enhance the electrical conductivity. This behaviour is different from that usually encountered in oxide solid solutions where the conductivity maximum is associated with the activation energy minimum [15]. The existence of a conductivity maximum is usually related to the variation of the charge carrier concentration and the electrostatic interactions between point defects [21], i.e. Al'_{Si} and O''_i in oxyapatites. A similar behaviour is more or less observed for the electrical grain boundary response.

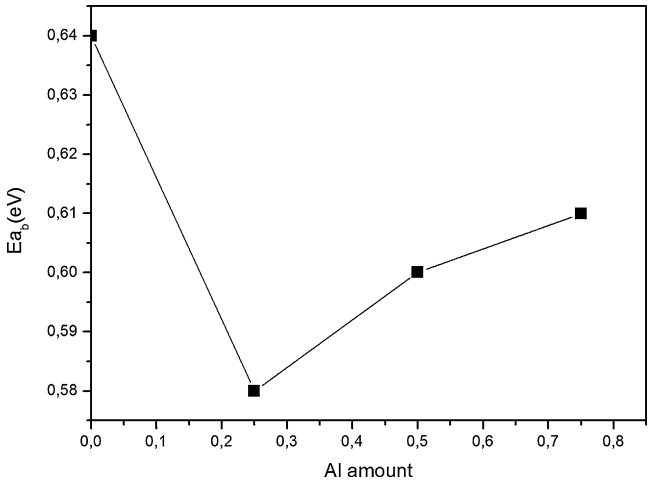

Fig. 7. Variation of the activation energy in the bulk as a function of Al-content at 350 °C.

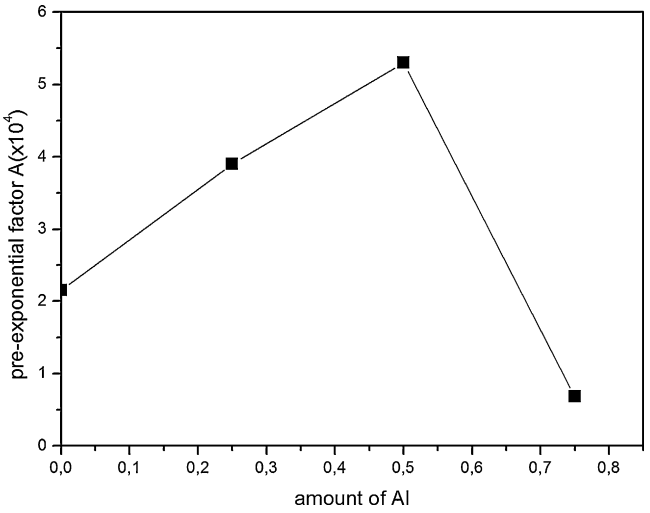

Fig. 8. Variation of the pre-exponential factor A in the bulk as a function of Al-content at 350 °C.

Within the (b) domain (500 °C ≤ T ≤ 790 °C), only the electrode response is accurately revealed in the impedance diagrams (see Fig. 9). Moreover one has access to the sum of the bulk and the grain boundary contributions but not to each of them separately. Consequently, in what follows, the electrical properties of the investigated oxyapatites will be discussed through the "total" (bulk + grain boundary) response. The main conclusions to be drawn are as follows:

The Arrhenuis plots of total conductivity are linear within the investigated temperature range. A similar behaviour was found by Shaula et al. [6] with activation energies close to 0.65 eV. This study shows also that Al-doping improves the oxyapatite conductivity (see Fig. 10). A conductivity maximum is observed for the sample containing 26.75 oxygen atoms per formula unit higher than that observed with YSZ (see Table 4). For the undoped sample $La_{9.33}Si_6O_{26}$, conductivity values determined in this work are different from those observed by Samson et al. [7]. The origin of this difference could be very likely attributed to the large difference in the sample densities, 67% and 91.8% (this work), respectively. Fig. 11 shows the variation of the total conductivity versus the oxygen partial pressure. No significant dependence is observed. These results are not sufficient to evaluate accurately the electronic part of conductivity. One

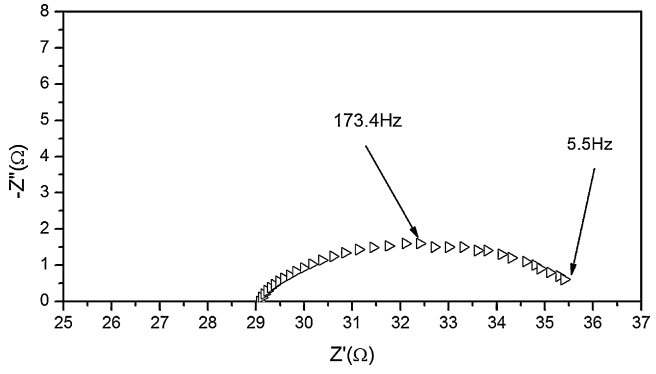

Fig. 9. Typical impedance diagram of $La_{10}Si_{5.5}Al_{0.5}O_{26.75}$ at 790 °C.

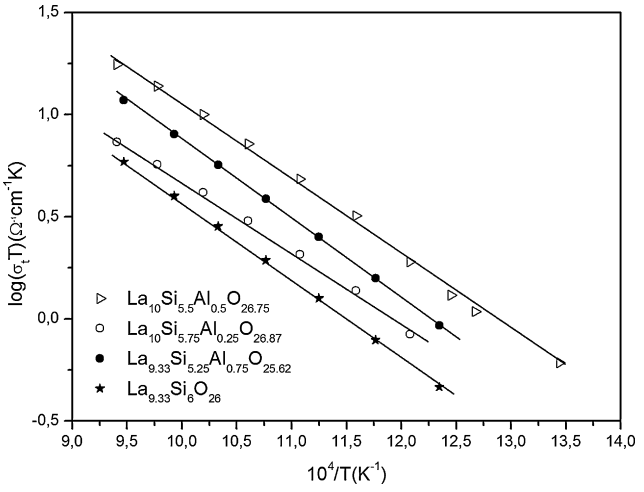

Fig. 10. Temperature dependence of the total conductivity of the investigated oxyapatites in air at high temperature.

Table 4
Total conductivity for different compositions

Sample composition	σ_{tot} (Ω^{-1} cm^{-1}) at 700 °C	Reference
$La_{9.33}Si_6O_{26}$	2.90×10^{-3}	This work
$La_{10}Si_{5.75}Al_{0.25}O_{26.87}$	5.70×10^{-3}	–
$La_{10}Si_{5.5}Al_{0.5}O_{26.75}$	1.01×10^{-2}	–
$La_{9.33}Si_{5.25}Al_{0.75}O_{25\cdot62}$	4.20×10^{-3}	–
8%mol YSZ	8.08×10^{-3}	[29]
$La_{9.33}Si_6O_{26}$	1.20×10^{-4}	[7]

may conclude that all the studied oxyapatites show a predominant ionic conductivity and could be used as solid electrolytes. However it must be noticed that the investigated samples are slightly pink coloured at high oxygen partial pressure, i.e. in air. This colour disappears in reducing atmosphere, i.e. in H_2–argon mixtures. One experimentally demonstrated that this colour phenomenon is reversible. Such a behaviour is usually attributed to the presence of colour centres within the solid phase involving lattice defects and electronic species.

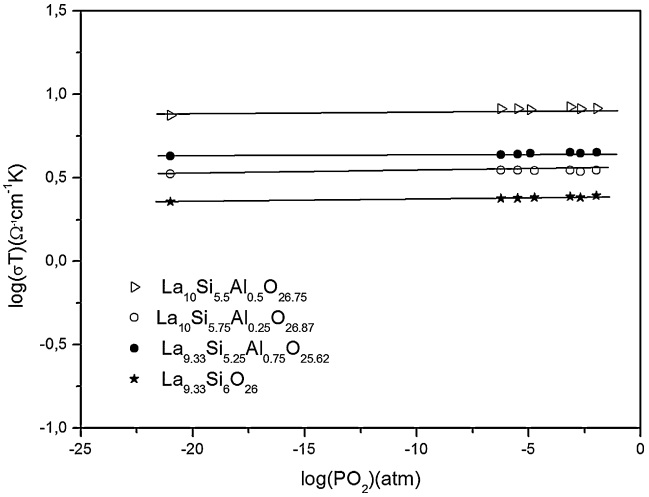

Fig. 11. Variation of the total conductivity versus PO_2 at 700 °C for oxyapatite ceramics.

As far as the conductivity mechanism in Al-doped oxyapatites is concerned, lowering charge on the tetrahedral sites in oxyapatites was already pointed out in literatures [8,22,23] implying local distortion of the SiO_4 tetrahedral group and thus greatly affecting the oxide migration. Several studies consider that migration of interstitial oxygen O_i'' is the major mechanism for ionic conductivity [9,24–27]. In oxyapatite, Islam et al. [28] has shown that a vacancy mechanism is characterized by a high activation energy (>1.1 eV) whereas oxygen interstitial migration is associated to lower activation energy, close to 0.7 eV [7,9,24]. Accordingly, our results seem to corroborate an interstitial mechanism in the investigated oxyapatites, O_i'' being the main charge carrier. Finally, the sample coloration observed at high oxygen partial pressure may be related to the p-type semiconduction measured by Shaula et al. [6] in the same group of oxyapatites. A study of the relation between these two factors can help to more clearly elucidate the electrical properties of oxyapatites.

4. Conclusion

This work has shown that the oxyapatites have ionic conductivities comparable if not higher than that of YSZ at intermediate temperature ($T < 800\,^{\circ}C$). No significant variation of conductivity is observed with changing of the oxygen partial pressure. Activation energy values favour an interstitial mechanism of ionic conduction by O^{2-}. Let us mention that recent Raman spectroscopy studies failed to identify the local modes of mobile species [30]. The possible use of these materials as solid electrolytes in the SOFC and in oxygen sensors implies

i) the search for an elaboration method at lower temperature,
ii) the study of their chemical and structural stability in the presence of electrodes and water vapour,
iii) the study of the evolution of their performances with time.

Part of this research is in progress in our laboratories.

Acknowledgements

This work was supported by the Ministry of higher education and scientific research of Tunisia and Rhône Alpes region. The authors would like to thank F. Roussel and S. Coindeau from CMTC for their fruitful help in the structural characterization respectively by MEB and DRX.

References

[1] V.V. Kharton, F.M.B. Marques, A. Atkinson, Solid State Ionics 174 (2004) 135–149.
[2] S.P.S. Badwal, K. Foger, Mater. Forum 21 (1997) 187–224.
[3] V.V. Kharton, A.L. Shaula, N.P. Vyshatko, F.M.B. Marques, Electrochim. Acta. 48 (2003) 1817–1828.
[4] S. Nakayama, M. Sakamoto, J. Eur. Ceram. Soc. 18 (1998) 1413–1418.
[5] J.E.H. Sansom, P.R. Slater, Solid State Ionics 167 (2004) 23–27.
[6] A.L. Shaula, V.V. Kharton, F.M.B. Marques, J. Solid State Chem. 178 (2005) 2050–2061.
[7] J.E.H. Sansom, D. Richings, P.R. Slater, Solid State Ionics 139 (2001) 205–210.
[8] E.J. Abram, D.C. Sinclair, A.R. West, J. Mater. Chem. 11 (2001) 1978–1979.
[9] P.R. Slater, J.E.H. Sansom, Solid State Phenom. 195 (2003) 90–91.
[10] H. Yoshioka, S. Tanase, Solid State Ionics 176 (2005) 2395–2398.
[11] A. Vincent, Thesis 2006, Tours University, France.
[12] Derek, J Zview, I. Scribner Associates Editor, 2005.
[13] C. Deportes, M. Duclot, P. Fabry, J. Fouletier, A. Hammou, M. Kleitz, E. Siebert, J. Souquet, Electrochimie des Solides, Presses Universitaires de Grenoble, 1994.
[14] J. Maier, J. Eur. Ceram. Soc. 24 (6) (2004) 1251–1257.
[15] R.E. Carter, W.L. Roth, in: C.B. Alcock (Ed.), Electromotive Force Measurements in High Temperature Systems, 1968, pp. 125–144.
[16] A. Madani, A. Cheikh, A. Touati, M. Labidi, H. Boussetta, C. Monty, Sens. Actuators B 109 (2005) 107–111.
[17] V.V. Kharton, A.P. Viskup, F.M. Figueiredo, E.N. Naumovich, A.A. Yaremchenko, F.M.B. Marques, Electrochim. Acta. 46 (2001) 2879–2889.
[18] S.H. Chu, M.A. Seitz, J. Solid State Chem. 23 (1978) 297–314.
[19] J.E. Bauerle, J. Phys. Chem. Solids 30 (1969) 2657–2670.
[20] T.Y. Tien, J. Appl. Phys. 35 (1964) 122–124.
[21] C.B. Alcock, in: C.B. Alcock (Ed.), Electromotive Force Measurements in High Temperature Systems, 1968, pp. 109–124.
[22] A. Najib, J.E.H. Sansom, J.R. Tolchard, P.R. Slater, M.S. Islam, Dalton Trans. 19 (2004) 3106–3109.
[23] L.L. Reina, J.M.P. Vazquez, E.R. Losilla, M.A.G. Aranda, Solid State Ionics 177 (2006) 1307–1315.
[24] S. Tao, J.T.S. Irvine, Mater. Res. Bull. 36 (2001) 1245–1258.
[25] J.R. Tolchard, M.S. Islam, P.R. Slater, J. Mater. Chem. 13 (2003) 1956–1961.
[26] V.V. Kharton, A.L. Shaula, M.V. Patrakeev, J.C. Warenborgh, D.P. Rojas, N.P. Vyshatko, E.V. Tsipis, A.A. Yaremchenko, F.M.B. Marques, J. Electrochem. Soc. 151 (2004) 1236–1246.
[27] S. Nakayama, Y. Higuchi, Y. Kondo, M. Sakamoto, Solid State Ionics 170 (2004) 219–223.
[28] M.S. Islam, J.R. Tolchard, P.R. Slater, Chem. Commun. (2003) 1486–1487.
[29] N. Takeda, Y. Itagaki, H. Aono, Y. Sadaoka, Sens Actuators B 115 (2006) 455–459.
[30] G. Lucazeau, N. Sergent, T. Pagnier, A. Shaula, V. Kharton, F.M.B. Marques, J. Raman Spectrosc. 38 (2007) 21–33.